How do Spatial Scale, Noise, and Reference Data affect Empirical Estimates of Error in ASAR-Derived 1 km Resolution Soil Moisture?

Marcela Doubková, Alena Dostálová (née Hegyiová), Albert I. J. M. van Dijk, Günter Blöschl, Wolfgang Wagner, *Senior Member, IEEE,* and Diego Fernández-Prieto

***Abstract*—The performance of the advanced synthetic aperture radar (ASAR) global mode (GM) surface soil moisture (SSM) data was studied over Australia by means of two widely used bivariate measures, the root-mean-square error (RMSE) and the Pearson correlation coefficient (R). By computing RMSE and R at multiple spatial scales and for different data combinations, we assessed how, and at which scales, the spatial sampling error, noise, and the choice of the reference data impact on RMSE and R. The results reveal large changes in RMSE and R with continental average values of 8% and 18% for the RMSE of relative soil moisture saturation and between 0.4 and 0.7 for R depending on the spatial scale of aggregation and the choice of reference data. The combined effect of noise and spatial sampling error accounted for a 79% RMSE increase at 1 km and predominated over the error due to the choise of the reference data also at 5 km scale. The effect of noise on RMSE strongly diminished at spatial scales ≥ 2 km. By contrast, the impact of uncertainties in the reference data was larger on R than on RMSE. This highlights the better potential of R to estimate the benefit of observations prior to data assimilation. Based on our results, it is further suggested that a potential way for an improved ASAR GM SSM error assessment is to: 1) aggregate the data to ≥ 2 km resolution to minimize the noise; 2) subtract the spatial sampling error within the coarse resolution footprint; and 3) remove the reference uncertainty using advanced techniques such as triple collocation.**

***Index Terms*—Advanced synthetic aperture radar global mode (ASAR GM), bivariate analyses, Pearson correlation coefficient, root-mean-square error (RMSE), soil moisture, synthetic aperture radar (SAR).**

Manuscript received October 30, 2013; revised February 16, 2014; accepted April 16, 2014. Date of publication June 16, 2014; date of current version November 04, 2014. This work was supported in part by the Austrian Science Fund (FWF) as part of the Doctoral Programme on Water Resource System (DK-plus W1219-N22) and in part by ESA SHARE-Extension2 (ESRIN/Contract no. 19420/05/I-EC) project.

M. Doubková was with the European Space Research Institute (ESRIN), 00044 Frascati, Italy. She is now with the Research Groups Photogrammetry & Remote Sensing, Vienna University of Technology (Technische Universität Wien), 1040 Wien, Austria (e-mail: marcela.doubkova@geo.tuwien.ac.at).

A. Dostálová and W. Wagner are with the Research Groups Photogrammetry & Remote Sensing, Vienna University of Technology (Technische Universität Wien), 1040 Wien, Austria (e-mail: alena.dostalova@geo.tuwien.ac.at; wolfgang.wagner@geo.tuwien.ac.at).

A. I. J. M. van Dijk is with the Fenner School of Environment & Society, The Australian National University, College of Medicine, Biology and Environment, Canberra ACT 0200, Australia (e-mail: albert.vandijk@anu.edu.au).

G. Blöschl is with the Institute of Hydraulic Engineering and Water Resources Management, Vienna University of Technology, A-1040 Wien, Austria (e-mail: bloeschl@hydro.tuwien.ac.at).

D. Fernández-Prieto is with the European Space Research Institute (ESRIN), 00044 Frascati, Italy (e-mail: diego.fernandez@esa.int).

Color versions of one or more of the figures in this paper are available online at http://ieeexplore.ieee.org.

Digital Object Identifier 10.1109/JSTARS.2014.2324657

I. Introduction

UNDERSTANDING errors in surface soil moisture (SSM) data is essential for assimilation of these data into models and blending SSM products from multiple satellite platforms [1]. The error is commonly estimated using bivariate measures [R, root-mean-square error (RMSE)] between the satellite SSM and a second SSM dataset derived by independent means. The latter is expected to be closer to the truth and hence referred to as the "reference" data. However, SSM is a notoriously ambiguous concept with high lateral and vertical variabilities that complicate a derivation of the true spatial SSM on ground. Moreover, the reference data often have different spatial resolutions from the evaluated SSM data. The error estimates thus not only reflect the random error and the conceptual discrepancies of the evaluated SSM product but are also inflated by errors due to: 1) spatial sampling; 2) bias between the evaluated and the reference data; and 3) uncertainty in the reference data related to the assumption that these data are free of error and represent the same quantity as the evaluated data.

Spatial sampling errors can originate from the assumption that a finer measure is representative of a larger resolution measurement or vice versa. This assumption is essentially wrong given the different causes for spatial variability between the point- and footprint-scale [2] and between different footprint sizes [3]. In particular, at small to medium resolutions ($100\ \mathrm{m}^{-1}$ km) soil moisture respond to variations in soil properties, vegetation, topography, radiation, and precipitation. At larger scales (>5 km), different sources of variation become apparent, such as climatic variations in precipitation or variations in humidity, temperature, and radiation that affect SSM through evapotranspiration. The impact of spatial sampling error was recently documented by Van der Velde *et al.* in [4] who used coarse resolution SSM acquisitions as a reference to evaluate advanced synthetic aperture radar (ASAR) wide swath (WS) fine resolution SSM. The authors concluded that the combined effect of spatial sampling error, noise, and bias explains more than 70% of the deviations between the two products.

Additionally, bivariate measures are affected by uncertainty in the reference data. Much attention has been recently given to understand the reference data uncertainty and to develop methods for its removal, such as triple collocation [5], [6]. Triple collocations studies, however, have focused on coarse resolution

data. To date, the assessment of the reference uncertainty when a variety of spatial resolutions is used in evaluation has not been explored.

In this study, the ASAR global mode (GM) SSM data developed through ESA DUE's SHARE [7] project are evaluated over the Australian continent using common bivariate measures (RMSE and R). An important contribution beyond previous studies is that we perform the analyses at multiple scales and with different choices for reference data. This helps to assess how, and at which scales, the spatial sampling error, ASAR GM noise, and the choice of the reference data impact on RMSE and R. As such, this study explores the impact of spatial scale and reference data (the "extrinsic errors" from here on) and noise when evaluating medium resolution SAR SSM products. The ASAR GM data used here cover the Australian during the ENVISAT's live time (2005–2012).

A number of previous evaluation studies demonstrated the ability of the data to capture soil moisture drying and wetting trends. These used an error propagation scheme [8], or comparison against *in situ* data [8], [9], or coarse (≥ 5 km) resolution SSM from models [10], or scatterometers [8]. The latter studies addressed the role of the ASAR GM SSM noise and its reduction via data averaging but did not investigate the role of spatial sampling error and error due to the uncertainty of the reference data.

In this study, first the spatial sampling error and noise are quantified over a smaller study area (1500×1500 km) in southeastern Australia using the spatial variance of the ASAR GM SSM within the coarser resolution (25 km) footprint as a proxy. The proportional share of noise in the latter is estimated by studying the differences between proxies computed using ASAR GM SSM with and without simulated random noise. Next, the effects due to spatial sampling error and noise are mapped over the entire continent. This is performed by computing the differences between RMSE maps acquired at finer (<5 km) and coarse (25 km) resolution ASAR GM. The important assumption is that the spatial variance differences between the ASAR GM 25 km aggregated product and the reference data can be neglected. Similarly, the effects due to choice of the reference dataset are studied by computing the difference maps between bivariate measures computed with different reference data. The coarse resolution data used were the Australian Water Resources Assessment landscape hydrological model (AWRA-L), ERA-Interim reanalyzes, and data from the Advanced Microwave Scanning Radiometer (AMSR-E). Finally, to allow for a comparison of effects due to separate error components, the differences are normalized by the 25-km RMSE and R maps.

Given the differences between the model conceptualization and the satellite acquisition the data do not necessarily represent the same time of the day. In particular, the ERA-Interim model runs at 3-hourly time step, the AWRA at a daily time step, and the ASAR GM and the AMSR-E acquisition produce soil moisture at the discrete time of acquisition. These differences in temporal support may introduce another additional source of (conceptual) error. This error is only marginally discussed in this study.

II. Data

A. ASAR GM SSM

The ASAR GM SSM represents the relative SSM in the upper <3 cm of soil and is retrieved from active radar sensor at the 1 km spatial resolution. Due to its high temporal sampling, the ASAR GM 1-km resolution sensor is suitable for monitoring of dynamical processes such as soil moisture [8] or inundation [11]. The ASAR GM data were retrieved using a change detection algorithm [8] assuming a sufficiently long time series to cover the full range of soil moisture values from wilting point to saturation [8], [13]. For the ASAR GM SSM product generation, a processing chain has been setup at the Vienna University of Technology (TU WIEN) [12]. The processing consists of a series of steps including geocoding, radiometric correction, resampling, normalization, and soil moisture retrieval [8], [10]. The resampling grid was defined in the Plate Carée map projection, based on the WGS84 datum with sampling distance of 0.00417° [12].

The algorithm was initially developed for ERS and ASCAT scatterometers [13]. Its transfer to ASAR GM was possible due to the very similar measurement principles of these instruments. Conversely, differences in spatial and radiometric resolution, polarization, and image retrieval geometry may limit the validity range of the transferred algorithm. The unit of the ASAR GM SSM product is the relative saturation level (%) and can be easily converted to the volumetric units by multiplying with porosity.

B. AWRA-L SSM

The AWRA-L SSM represents the relative SSM in the upper 5–10 cm of soil. The AWRA-L hydrological model [14] is a part of the AWRA [15] system that consists of a selection of models that estimate all water balance terms associated with the vegetation, soil, groundwater, and surface water balance. The AWRA-L SSM data are available at daily time step and computed at 0.05° grid resolution (ca. 5 km) across the Australian continent.

To avoid uncertain and equivalent soil parameters [16], the separate soil layers in the AWRA-L model are defined not in terms of soil layer thickness but in terms of their extractable water storage capacity [14]. Relevant here is that the model structure is based on the assumption that any water in excess of field capacity drains within a day (in other words, soil moisture content never exceeds field capacity). This simplification was made because the model is designed to provide information of soil water availability and average storage changes over longer periods (e.g., months). It will be demonstrated that this simplifying assumption affects the comparison with remotely sensed SSM. The main difference between the AWRA-L units and the volumetric soil moisture is that volumetric soil moisture allows values above field capacity and below saturation, whereas AWRA-L units do not. The main input data to the model are precipitation, short wave radiation, and temperature data derived by interpolation from data from a national network of climate station at 0.05°. In this study, SSM estimates from AWRA version 0.5 were used; the same data used by [10] and [17].

C. AMSR-E SSM

The AMSR-E SSM represents the volumetric soil moisture in the upper <3 cm of soil. The data are retrieved at the original footprint of 56 km and resampled to 0.25° spatial resolution. The brightness temperatures measured by the AMSR-E were converted to volumetric soil moisture using the Land parameter Retrieval Model [18]. The method uses a forward modeling optimization procedure to solve a radiative transfer equation for both soil moisture and vegetation optical depth. The AMSR-E soil moisture derived from the C-band was used in this study, as this is expected to represent soil depth corresponding to that represented by the ASAR GM soil moisture product. Only night-time acquisitions were used, as these were better suited for retrieving soil moisture than day-time observations [19].

D. ERA-Interim SSM

The ERA-Interim SSM represents simulations of soil moisture in the upper approximately 0–7 cm of soil at approximately 80 km spatial resolution. The data are freely available at http://apps.ecmwf.int/datasets/. The ERA-Interim reanalysis (both atmosphere and surface parameters) is based on the ECMWF Integrated Forecast System (IFS) model [20] using a sequential data assimilation scheme. In each cycle, available observations are combined with prior information from a forecast model to estimate the evolving state of the global atmosphere and its underlying surface [21]. The variety of satellite and ground-based measurements assimilated include, among others, clear-sky radiance, rain-affected SSM/I radiances, or recalibrated ERS-1 and ERS-2 surface wind data. It should be noted that the data used here do not involve assimilation of scatterometer over land. The land surface processes in IFS are described by the Tiled ECMWF Scheme for Surface Exchanges over Land (TESSEL) in four layers [22] using a globally uniform soil type with fixed soil hydraulic parameters with saturation value of $0.472\ \mathrm{m^3m^{-3}}$, field capacity with $0.323\ \mathrm{m^3m^{-3}}$, and the wilting point with $0.171\ \mathrm{m^3m^{-3}}$.

III. Methodology

A. Data Processing

For the purpose of this study, more than 7000 ASAR GM scenes over Australia were processed using all available acquisitions between January 1, 2005 and January 31, 2010. Next, three SSM data (ERA-Interim, AWRA-L, and AMSR-E; the "reference data" from here on) were obtained for the identical dates to those of the ASAR GM SSM. The data were assumed to have independent errors (see Section III-D for discussion).

Remotely sensed and modeled SSM data may represent different soil moisture depths, different spatial footprints ("spatial support" sensu [3]), and have different statistical moments [23]. This inevitably introduces biases that preclude determination of the absolute agreement between SSM time series and data assimilation into models [24]. Commonly applied approaches for biases removal are transformation using linear regression or the cumulative distribution function (CDF) [23]. In this study, the linear regression technique was used. The decision was driven by the fact that only slight differences in the absolute RMSE values were found when different matching techniques were used and that only at 5 and 25 km scale (not displayed). Furthermore, linear regression is computationally less expensive, allows tracking back the computation more directly than CDF and does not change the Pearson correlation coefficient. It should be, however, noted that other matching techniques may be more appropriate if other reference or evaluated data are used.

The linear regression removes not only the differences in statistical moments but also differences in SSM units (Table I). This is relevant given the expected linear relationship between the separate SSM units [17], [25]. Given the purpose of this study to evaluate the quality of the ASAR GM SSM, the reference data were transformed to the ASAR GM SSM data. In all subsequent computations, the transformed and bias-corrected AWRA-L, ERA-Interim, and AMSR-E data were used. Importantly, the fitting was performed separately for each ASAR GM aggregation level.

Next, only acquisitions coinciding in time in all the four data were selected using a maximal temporal difference of 12 h. This selection was controlled by the irregular acquisitions of the ASAR GM and by the fact that only night-time acquisitions from AMSR-E were used. The used amount of acquisition quartets is shown in Fig. 1.

TABLE I
An Overview of Used SSM Data and Their Original Units Prior to Data Transformation Using Linear Regression (See Section III)

Data	Unit	Layer depth (cm)	Spatial resolution (km)	Temporal resolution
ASAR GM	Relative saturation level (%)	< 3	1	Irregular, every 2-3 days on average
AWRA-L	% of available water content at field capacity	5–10	0.05° (ca. 5)	Daily
AMSR-E	Volumetric (m^3m^{-3})	< 3	0.25° (ca. 25)	Daily
ERA-Interim	Volumetric (m^3m^{-3})	Approx. 7	80	Daily

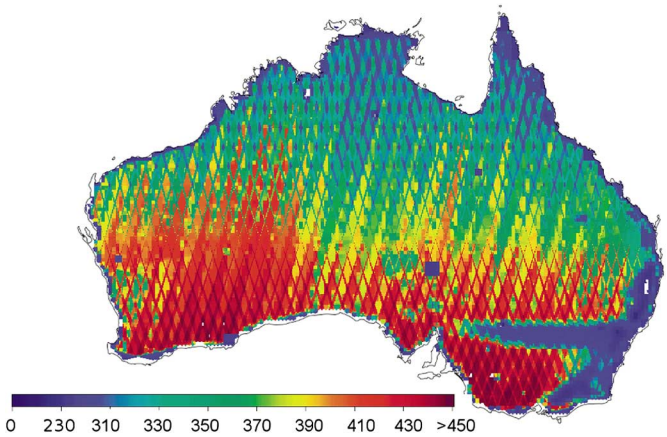

Fig. 1. Number of ASAR GM SSM acquisitions per pixel used in this study. The map is shown at 5 km spatial resolution.

B. Evaluation Measures

The $\mathrm{RMSE_{r,j}}$ signifies the closeness of ASAR GM SSM ($\theta_{S,i,j}$) to the reference data ($\theta_{R,i,j}$) as follows:

$$RMSE_{r,j} = \sqrt{\frac{\sum_{i=1}^{N}\left(\theta_{S,i,j} - \theta_{R,i,j}\right)^2}{N}} \quad (1)$$

where $i = 1 \ldots, N$ and N is the number of days with available acquisitions, r represents the reference data, and j stands for the spatial scale (1, 5, and 25 km, respectively). The squaring is performed to remove the potential negative value and quadratically penalizes the residuals between ASAR GM and the reference SSM.

The Pearson correlation coefficient $R_{r,j}$ measures linear relationship between ASAR GM SSM ($\theta_{S,i,j}$) and the reference data ($\theta_{R,i,j}$) as follows:

$$R_{r,j} = \frac{\frac{1}{N}\sum_{i=1}^{N}\left(\theta_{S,i,j} - \overline{\theta_{S,j}}\right)\left(\theta_{R,i,j} - \overline{\theta_{R,j}}\right)}{\sqrt{\frac{1}{N}\sum_{i=1}^{N}\left(\theta_{S,i,j} - \overline{\theta_{S,j}}\right)^2 \frac{1}{N}\sum_{i=1}^{N}\left(\theta_{R,i,j} - \overline{\theta_{R,j}}\right)^2}} \quad (2)$$

where $\overline{\theta_{S,j}}$ is the mean of all $\theta_{S,i}$ and $\overline{\theta_{R,j}}$ is the mean of all $\theta_{R,i}$ for a given spatial scale j. The important difference between the two evaluation measures is that RMSE describes the absolute correspondence of two data while R refers to the correspondence of anomalies computed with respect to the one to one linear relationship.

The evaluation measures were computed at three spatial scales—1, 5, and 25 km—that are nearly identical to 0.01, 0.05, and 0.25 ° for Australia. The scales were selected to address the spatial scales at which the data quality is often required, ranging from moderate resolution hydrological models to coarse resolution atmospheric models. The ASAR GM and the biases-corrected reference data were over-sampled and aggregated to correspond to the three spatial scales. The nearest neighbor method was used to over-sample the reference data, whereas the linear aggregation was applied to the ASAR GM SSM and to the AWRA-L, when aggregating to the 25 km. The aggregation of the ASAR GM SSM was performed over areas with at least 30% coverage (the ASAR GM has an irregular orbit that may result in an incomplete coverage of the aggregated footprints). The remaining areas were marked with a missing value.

The result was presented in nine maps for both evaluation measures, RMSE and R. These are in the text indexed with AW, AM, and AE referring to the used reference data AWRA-L, AMSR-E, and ERA-Interim, respectively and with 1, 5, or 25 that refers to the different spatial resolutions. The results were also shown in form of box plots summarizing median, median, minimum, maximum, and 25th and 75th percentiles for each map using only pixels with significant correlation between ASAR GM and the reference data. The minimum and maximum values were treated for outliers by removing the 1st and the 99th percentiles of the data, respectively.

C. Quantifying Impact of Extrinsic Errors and Noise on RMSE

First, we quantified the spatial sampling error and the ASAR GM noise on RMSE over a smaller study area (1500×1500 km) in southeastern Australia assuming that the spatial variance differences between the ASAR GM 25 km aggregated product and the reference coarse resolution products can be neglected given their alike spatial resolutions. This assumption is relevant also for medium resolution AWRA-L, as the spatial variances of AWRA-L at 5 and 25 km was alike (not shown). Under this assumption, we could estimate the spatial sampling error and the ASAR GM noise at variety of spatial scales ranging between 1 and 25 km and using the spatial variance of ASAR GM ($\mathrm{RMSE_{AS}}$) as a proxy as

$$RMSE_{AS,j} = \sqrt{\frac{\sum_{i=1}^{N}\left(\theta_{S,i,j} - \theta_{S,i,25}\right)^2}{N}} \quad (3)$$

where $\theta_{S,i,25}$ represents the aggregated 25 km ASAR GM and $\theta_{S,i,j}$ represents the finer resolution ASAR GM SSM with j aggregation level ranging between 1 and 25 km. Similar quantification was performed in [26] to correct for the spatial sampling error of a soil moisture network.

Second, the ASAR GM data are affected by a high level of noise that is expected to have a significant impact on RMSE [8]. To assess the significance of this effect, (3) was computed twice: 1) once using the actual ASAR GM data and 2) once using the ASAR GM data with simulated random noise added. The simulated noise with normal (Gaussian) distribution was used with $\sigma = 10\%$ and $\sigma = 20\%$ of relative soil moisture, respectively. The σ's were selected to describe the expected impact of the estimated ASAR GM noise level of ~ 1.2 dB on the dynamic range of the ASAR GM backscatter measurements over Australia (6–18 dB). In addition, the impact of noise on RMSE was assessed by studying the change of variance σ_j^2 with the increasing aggregation level. The σ_j^2 was computed as

$$\sigma_j^2 = \frac{\sum_{i=1}^{N}\left(\theta_{S,i,j} - \overline{\theta_{S,j}}\right)^2}{N} \quad (4)$$

with aggregation level j ranging between 1 and 80 km.

Third, to demonstrate the spatial impact on RMSE due to the spatial sampling error and the ASAR GM noise over the entire continent, we subtracted maps acquired at finer spatial resolutions from those acquired at coarse spatial resolutions while keeping the reference data identical. This is expressed as

$$\Delta sRMSE_{r,j} = RMSE_{r,j} - RMSE_{r,25}. \quad (5)$$

Fourth, the evaluation measures are impacted by the uncertainty of the reference data. To assess how the choice of the reference data impact RMSE, the continental maps acquired using different coarse resolution reference data were subtracted while keeping the spatial resolution identical. This is expressed as

$$\Delta rRMSE_{r-(r+1),j} = RMSE_{r,j} - RMSE_{r+1,j}. \quad (6)$$

Simply, $\mathrm{\Delta rRMSE_{r-(r+1),j}}$ measure expresses how much RMSE differs under the influence of two independent reference uncertainties, whereas $\mathrm{\Delta sRMSE_{r,j}}$ expresses how much RMSE differ due to spatial sampling error and ASAR GM noise.

Fifth, the overall impact on RMSE was quantified that occurred due to: 1) the spatial sampling error and noise and 2) the choice of the reference data. The average percentage impact on RMSE due to the spatial sampling error and noise was computed as an average normalized $\Delta\mathrm{sRMSE_j}$ as

$$n\Delta sRMSE_j = \frac{1}{3}\left(\sum_r^3 \frac{\Delta sRMSE_{r,j}}{RMSE_{r,25}}\right) * 100. \quad (7)$$

The normalization of RMSE with the 25-km RMSE was motivated by the assumption that the spatial sampling error at 25 km scale can be neglected. In addition, the normalization to 25 km RMSE allows for comparison of different error contributions. The normalized change due to the choice of the reference data was computed as

$$n\Delta rRMSE_j = \frac{1}{3}\left(\sum_r^3 \frac{\Delta rRMSE_{r-(r+1),j}}{RMSE_{r,25}}\right) * 100. \quad (8)$$

D. Quantifying Impact of Extrinsic Errors and Noise on R

The quantification of the extrinsic errors and noise on R closely follows the quantification of the errors on RMSE in (3)–(8). First, the spatial sampling correlation (R) was calculated according to

$$R_{AS,j} = \frac{\frac{1}{N}\sum_{i=1}^{N}\left(\theta_{S,i,j} - \overline{\theta_{S,j}}\right)\left(\theta_{S,i,25} - \overline{\theta_{S,25}}\right)}{\sqrt{\frac{1}{N}\sum_{i=1}^{N}\left(\theta_{S,i,j} - \overline{\theta_{S,j}}\right)^2 \frac{1}{N}\sum_{i=1}^{N}\left(\theta_{S,i,25} - \overline{\theta_{S,25}}\right)^2}} \quad (9)$$

where $\overline{\theta_{S,25}}$ is the mean of all $\theta_{S,i,25}$. The measure $1 - R_{AS,j}$ identifies the decrease from maximum $R = 1$ due to spatial sampling error and ASAR GM noise. Inversely to $\mathrm{RMSE_{AS}}$, the $\mathrm{R_{AS}}$ increases with the increasing ASAR GM aggregation level.

Next, the significance of the effect of noise on R was assessed by computing (9) twice: 1) using the actual ASAR GM data and 2) using the ASAR GM data with added simulated random noise [normal (Gaussian) distribution with $\sigma = 10\%$ and $\sigma = 20\%$, respectively].

To map the change in R due to the spatial sampling error over the entire continent, we, similarly to (5), subtracted R maps at different spatial scales as

$$\Delta sR_r = R_{r,25} - R_{r,j}. \quad (10)$$

The effect due to the choice of the reference data was quantified, similarly as in (6) for RMSE, according to

$$\Delta rR_{r-(r+1),j} = R_{r,j} - R_{r+1,j}. \quad (11)$$

Finally, the overall impact due to: 1) the spatial sampling error and noise and 2) the choice of the reference data on R was expressed, similarly as in (7) and (8), by

$$n\Delta sR_j = \frac{1}{3}\left(\sum_r^3 \frac{\Delta sR_{r,j}}{R_{r,25}}\right) * 100 \quad (12)$$

and

$$n\Delta rR_j = \frac{1}{3}\left(\sum_r^3 \frac{\Delta rR_{r-(r+1),j}}{R_{r,25}}\right) * 100. \quad (13)$$

The subtraction method does not enable the actual quantification of the spatial sampling error, noise, and reference uncertainty because R and RMSE are not additive measures. It, however, does provide an estimate if and how RMSE and R differ under influence of different sampling error, noise, and choice of reference data. The method can be applied under the assumption that the errors of the reference data are independent. This assumption seems reasonable; the ASAR GM backscatter, the AMSR-E brightness temperatures as well as the input data to the AWRA-L and ERA-Interim model are all likely to be independent from each other. The ASAR GM and AMSR-E data are perhaps most likely to have dependent errors due to some similarities in the physics of the retrieval, but previous studies have shown that the retrievals errors have very different spatial patterns and, therefore, can probably be assumed independent [5].

IV. Results and Discussion

A. Impact of Extrinsic Errors and Noise on RMSE

The RMSE between the ASAR GM SSM and three reference data are shown in Fig. 2 and summarized in boxplots in Fig. 3. At 1 km, the three maps with different references exhibit very similar spatial patterns. The high $\mathrm{RMSE_{r,1}}$ values ($>22\%$) dominate over vegetated (darker brown color in Fig. 2) and topographically complex areas and can be explained by the limited sensitivity of the ASAR GM data to the soil moisture dynamics due to the vegetation attenuation and by the limited soil moisture dynamics over outcrop areas with missing soil layer. This supports the findings of [10] who found a high correspondence of RMSE and ASAR GM SSM propagated error at 1 km spatial resolution and concluded that at 1 km, RMSE primarily reflects the random error and noise of the ASAR GM SSM. The areas in the croplands in the southeastern and southwestern Australia show RMSE values of 16%–22%. The lowest $\mathrm{RMSE_{r,1}}$ values ($<16\%$) are found in the arid and semiarid grassland and open woodland areas ([10], Figs. 2 and 3) where soil moisture variations are small.

The $\mathrm{RMSE_{r,5}}$ and $\mathrm{RMSE_{r,25}}$ are noticeably different from $\mathrm{RMSE_{r,1}}$. Both absolute and relative changes when compared to $\mathrm{RMSE_{r,1}}$ are apparent and are probably related to the spatial sampling error and the decrease of the ASAR GM noise. There is only a slight decrease from $\mathrm{RMSE_{r,5}}$ to $\mathrm{RMSE_{r,25}}$. In particular, the 18% median $\mathrm{RMSE_{r,1}}$ decreases to 12% for $\mathrm{RMSE_{r,5}}$ and further to 10% for $\mathrm{RMSE_{r,25}}$ (Fig. 3). Also, the high contrasts between the $\mathrm{RMSE_{r,1}}$ values in eastern and northern Australia (brownish to green patches in Fig. 2) are reduced at 5 and 25 km scales. At coarser resolutions (≥ 5 km), the differences between maps computed with different references become more evident and will be in detail discussed later in this section. A good example of this can be found in northeastern Australia where

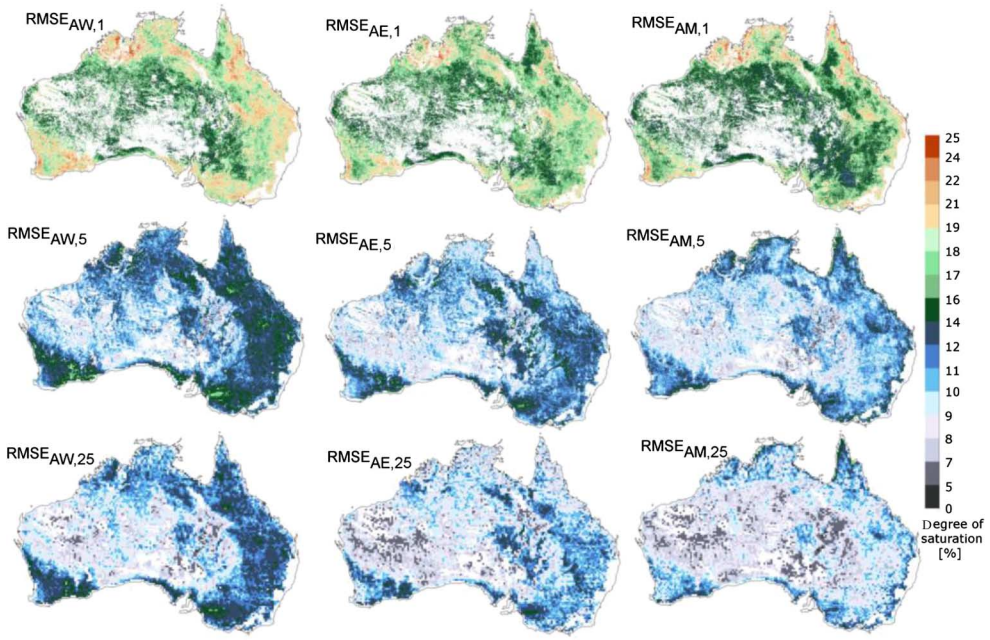

Fig. 2. RMSE computed between ASAR GM and AWRA-L SSM ($\mathrm{RMSE_{AW}}$) (left), ERA-Interim ($\mathrm{RMSE_{AE}}$) (center), and AMSR-E SSM ($\mathrm{RMSE_{AM}}$) (right). The analyses were performed at 1 (upper line), 5 (center line), and 25 (lower line) km scale. The white areas show the nonsignificant correlation values ($\mathrm{p} > 0.05$) or missing values. The units represent the degree of saturation (%).

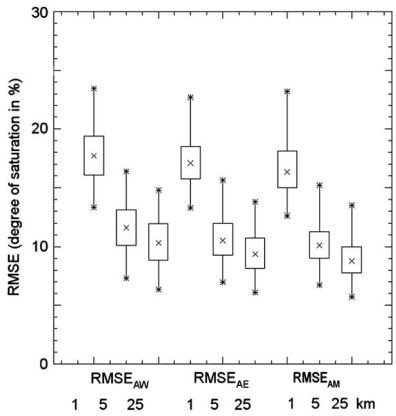

Fig. 3. Box-plot representation of quantities of the RMSE maps computed from Fig. 2. The boxes show the median, 25th and 75th percentiles; the crosses represent the minimum and maximum RMSE after outliers were removed.

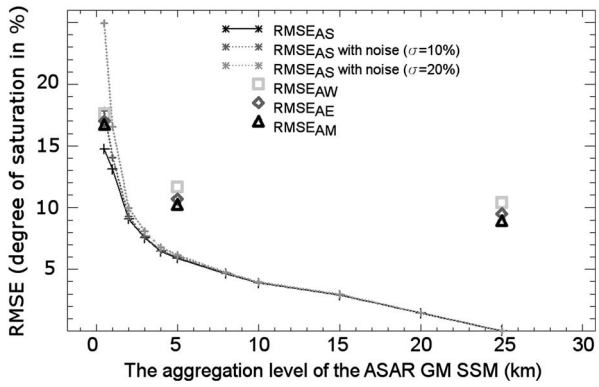

Fig. 4. Assessment of the spatial sampling errors, approximated by $\mathrm{RMSE_{AS}}$, with the increasing ASAR GM SSM aggregation (3) over 1500 by 1500 km area in southeastern Australia without (black line) and with introduced random noise ($\sigma = 10\%$ and $\sigma = 20\%$) (gray lines), overlaid with continental mean of $\mathrm{RMSE_{AE}}$, $\mathrm{RMSE_{AW}}$, and $\mathrm{RMSE_{AM}}$.

$\mathrm{RMSE_{AE,5}}$ and $\mathrm{RMSE_{AW,5}}$ values remain above 12%, whereas $\mathrm{RMSE_{AM,5}}$ shows values below 9%. Even, larger differences are apparent between the three $\mathrm{RMSE_{r,25}}$ maps.

Fig. 3 summarizes the statistical quantities from Fig. 2 and depicts the large decline in values between the RMSE maps computed at different ASAR GM aggregation levels as well as the lesser differences between RMSEs computed with different reference data.

Next, the spatial sampling error and noise were estimated according to (3) using $\mathrm{RMSE_{AS,j}}$ as a proxy. The $\mathrm{RMSE_{AS,j}}$ logarithmically decreases with increasing aggregation j of ASAR GM SSM (Fig. 4). This corresponds to decrease of $\mathrm{RMSE_{r,j}}$ (computed using a reference dataset according to (1) and overlaid onto Fig. 4) and suggests a strong effect of sampling error and noise on RMSE at medium scales (≤ 5 km). At coarser resolutions, $\mathrm{RMSE_{AS,j}}$ decreases more rapidly than $\mathrm{RMSE_{r,j}}$ suggesting the impact of reference uncertainty on $\mathrm{RMSE_{r,j}}$ at coarser resolutions.

The above-mentioned analyses quantified the combination of sampling error and noise. To estimate which portion of $\mathrm{RMSE_{AS,j}}$ is impacted by noise we computed $\mathrm{RMSE_{AS}}$ again, this time with simulated random noise with $\sigma = 10\%$ and $\sigma = 20\%$ relative saturation level, respectively (gray lines in Fig. 4). The impact on RMSE at the original ASAR GM resolution is on average 3% and 10% of relative soil moisture saturation level, respectively. The noise decreases with the aggregation level of ASAR GM and significantly impacts RMSE up to a spatial scale of 2 km. As a result, at spatial scales ≥ 2 km, $\mathrm{RMSE_{AS}}$ can be assumed to represent dominantly the sampling error.

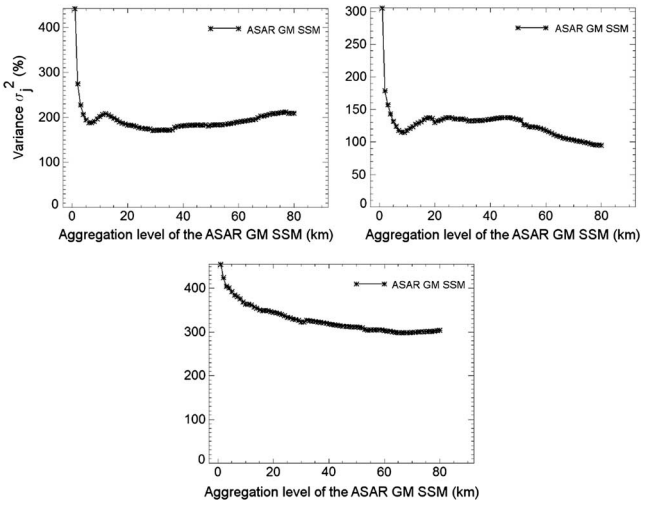

Fig. 5. Variance σ_j^2 of the ASAR GM computed at different aggregation levels at three locations: $\mathrm{lon} = 143$, $\mathrm{lat} = -18.5$ (upper left), $\mathrm{lon} = 131$, $\mathrm{lat} = -23.5$ (upper right), and $\mathrm{lon} = 145$, $\mathrm{lat} = -35.5$ (below).

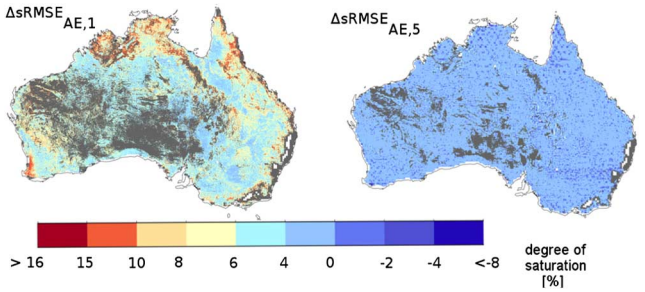

Fig. 6. Impact of the spatial sampling error and ASAR GM noise on $\mathrm{RMSE_{AE}}$ as computed in (5). The gray areas correspond to the nonsignificant correlation values ($\mathrm{p} > 0.05$) or missing values. The units represent the degree of saturation (%).

The impact of noise on RMSE can also be studied by assessing the change in the ASAR GM variance σ_j^2 (4) at different aggregation levels (Fig. 5). The change in variance is expected to be composed of variation due to different atmospheric and land surface processes and follow a power law as a function of the aggregated area [27], [28]. Superimposed on this variation is the variation due to the ASAR GM noise. The decrease at medium scales (≤ 5 km) is rapid and attributed to the decreasing noise level rather than large scale SSM variations related to land and atmospheric processes that dominate at coarser aggregation levels. The length scale of the decrease of variance at medium scales is shorter for wet (Fig. 5, above left and below) than for dry SSM conditions (Fig. 5, above right). Nevertheless, the most significant decrease in variance occurs at spatial scales ≤ 2 km, which corresponds to our findings from the simulated noise experiment in Fig. 4.

Next, we spatially estimated the impact of the spatial sampling error and noise on RMSE by subtracting maps calculated at varying spatial resolutions (5). Maps using the ERA-Interim reference data are shown in Fig. 6 ($\Delta\mathrm{sRMSE_{AE,1}}$ and $\Delta\mathrm{sRMSE_{AE,5}}$). It is noted that this analysis does not provide an estimate of error itself, but its effect on RMSE. The larger difference between $\mathrm{RMSE_{AE,1}}$ and $\mathrm{RMSE_{AE,5}}$ maps when compared with the $\mathrm{RMSE_{AE,5}}$ and $\mathrm{RMSE_{AE,25}}$ maps are caused by the spatial sampling error and ASAR GM noise present at medium resolutions that rapidly decrease toward 5 km (Fig. 4). Difference maps using other alternative reference data (i.e., AMSR-E and ERA-Interim) were very similar to those in Fig. 6 (not shown). This correspondence supports our assumption that the difference method (5) mainly shows the effect of spatial sampling error and is not strongly impacted by reference data uncertainty.

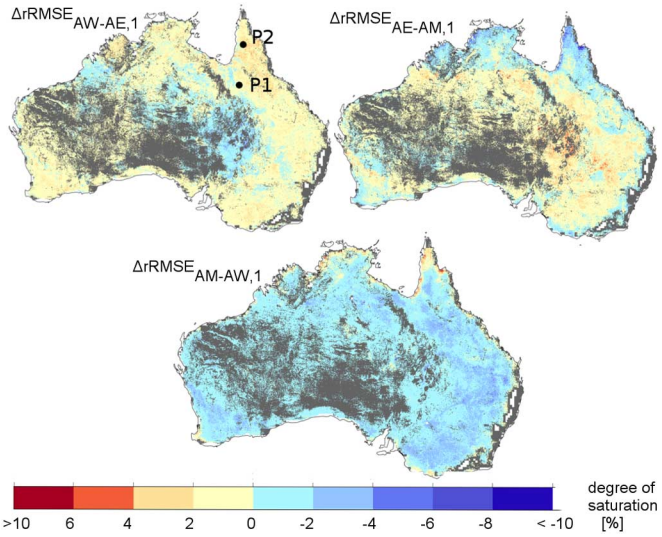

Fig. 7. Impact of the selection of the reference data on RMSE at 1 km resolution as computed in (6). The gray areas correspond to the nonsignificant correlation values ($\mathrm{p} > 0.05$) or missing values.

To spatially estimate the impact due to the choice of reference data, difference maps were computed between RMSE acquired from different reference data (6) (Fig. 7). The difference maps computed at coarser resolutions showed very similar spatial patterns but different absolute values (not shown). The $\mathrm{RMSE_{AM,1}}$ values are the lowest. This can be explained by the high radiometric quality of the product, by the similarities in the physics of both the AMSR-L and ASAR GM product and by the similar represented depth of the active and passive microwave soil moisture data.

The low uncertainty values of AMSR-E product over majority of the continental land with an exception of the coastal areas correspond to the findings of [29]. Also, over vast portion of Australia, $\mathrm{RMSE_{AW,1}}$ values are larger than $\mathrm{RMSE_{AM,1}}$ and $\mathrm{RMSE_{AE,1}}$. The higher $\mathrm{RMSE_{AW,1}}$ is explained by the fact that the AWRA-L model assumes that the soil drains to field capacity within a day and thus simulated SSM never exceeds field capacity [14]. By contrast, ERA-Interim data allow values between field capacity and saturation as it simulates drainage of wet soil (above field capacity) over 30-hourly time steps. Similarly, the physically based algorithm of the AMSR-E allows values above field capacity.

The above-mentioned properties of the AWRA-L dataset are further illustrated by time series of AWRA-L and ERA-Interim for selected locations (Fig. 8). At Point 1, the ERA-Interim top soil layer dries out rapidly and reaches a stable low value that is not realistic when compared with the observations. By contrast, AWRA SSM reproduces the longer continuing dry-down better,

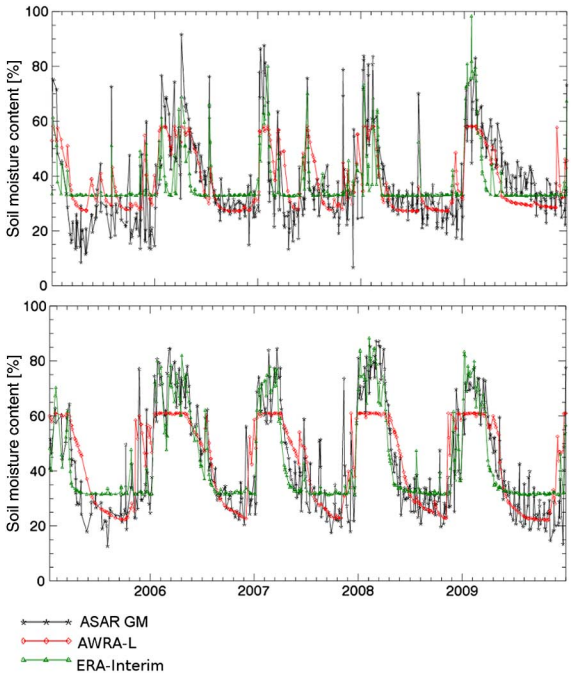

Fig. 8. Time series of ASAR GM, AWRA-L, and ERA-Interim SSM over 5×5 km large areas P1 (above) and P2 (below). The location of the areas is shown in Fig. 7.

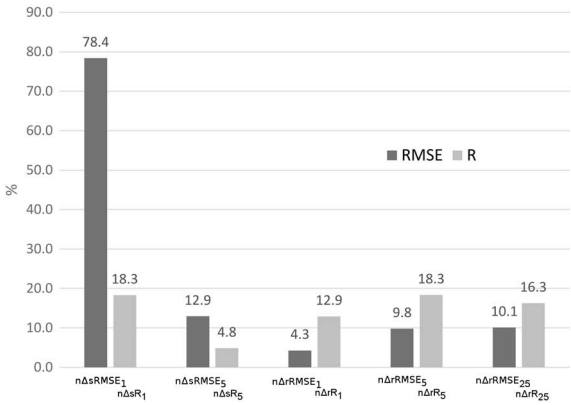

Fig. 9. Impact on RMSE and R (%) due to the aggregation of the ASAR GM SSM ($\mathrm{n}\Delta\mathrm{sRMSE}$ and $n\Delta sR$) and due to the choice of the reference data ($\mathrm{n}\Delta\mathrm{rRMSE}$ and $n\Delta rR$). The indices were computed according to (7), (8), (12), and (13).

but remains stable at field capacity for prolonged periods during the wet season (especially at Point 2) because of the mentioned simplifications in the model. Conversely, ERA continues to show variations that are more realistic when compared with the observations. In addition, the differences at relatively high values at Point 2 impact the final RMSE stronger than the differences at relatively low values at Point 1 resulting in RMSE over Point 2 to be higher. A single RMSE hides this complexity. It should further be noted that the differences between RMSE maps may also relate to the different depths (Table I) that the respective reference data represent.

In the final step, the impacts of the spatial sampling error, noise, and reference data were quantified as in (7) and (8) and their continental means are shown in Fig. 9. The effect due to the spatial sampling error and noise $\mathrm{n}\Delta\mathrm{sRMSE}$ accounted on average for 79% of RMSE at 1 km and to about 13% of RMSE at 5 km. The large impact of the spatial sampling error and noise correspond to the results of Van der Velde *et al.* [4] who found that up to 70% of RMSE can be explained with bias and deviations in scale differences. The continental average of $\mathrm{n}\Delta\mathrm{rRMSE}$ was 4.3% at 1 km resolution and increased, as the spatial sampling error and noise decreased, to 9.8% and 10.1% at 5 and 25 km spatial resolution, respectively. It suggests that the effect of extrinsic errors and noise is large and should be accounted for prior to application of the ASAR GM data. Based on our results, it is suggested that a potential way to do is to: 1) aggregate the data to ≥ 2 km resolution to minimize the noise; 2) subtract the spatial sampling error within the coarse resolution footprint (e.g., using $\mathrm{RMSE}_{\mathrm{AS}}$ as a proxy) as performed in [26] for a soil moisture network; and 3) remove the reference uncertainty using more advanced techniques such as triple collocation [5].

It is reiterated that the RMSE maps are influenced by the bias correction method applied. Different matching techniques can impact the results locally and need to be further investigated. In addition, soil moisture from models and from remote sensing typically exhibit very different mean and variability [23]. Hence, further investigation on differences in RMSE maps if all data are bias corrected with respect to the reference data could lead to additional insights.

B. Impact of Extrinsic Errors and Noise on R

The R maps between the ASAR GM SSM and the three reference data are shown in Fig. 10 and their statistical properties are summarized in Fig. 11. The R maps show very similar spatial patterns to RMSE with high (>0.6) over areas with large total rainfall or sparse vegetation and the low over arid and semiarid areas.

Clearly, $R_{r,j}$ increases with the increasing scale of aggregation of the ASAR GM SSM product. It is noted that the same aggregation caused an exponential decrease of $\mathrm{RMSE}_{\mathrm{r,j}}$ (Fig. 3). Apparently, the sensitivity of R to the spatial sampling error and noise is lower than the sensitivity of RMSE. This may be explained by the fact that RMSE quadratically penalizes residuals between model and observations, whereas the computation of R limits the effect of the residuals by computing the covariance, in other words detecting the correspondence of anomalies computed with respect to the one to one linear relationship. This supports the earlier findings with the ASAR WS radar backscatter that showed that despite the high variability in the temporal domain soil moisture measured at specific locations is correlated to the mean soil moisture content over an area [30].

Fig. 11 shows the increase of $R_{r,j}$ with decreasing spatial sampling error and noise for different reference data. In contrast to RMSE (Fig. 3), differences in R values due to the choice of the reference data are larger than due to increasing aggregation levels. The largest change in R due to the choice of the reference data was 0.17 (between $\mathrm{RMSE}_{\mathrm{AW,25}}$ and $\mathrm{RMSE}_{\mathrm{AM,25}}$), whereas the largest improvement with coarsening spatial resolution reached only 0.13 ($\mathrm{RMSE}_{\mathrm{AM,1}}$ and $\mathrm{RMSE}_{\mathrm{AM,25}}$).

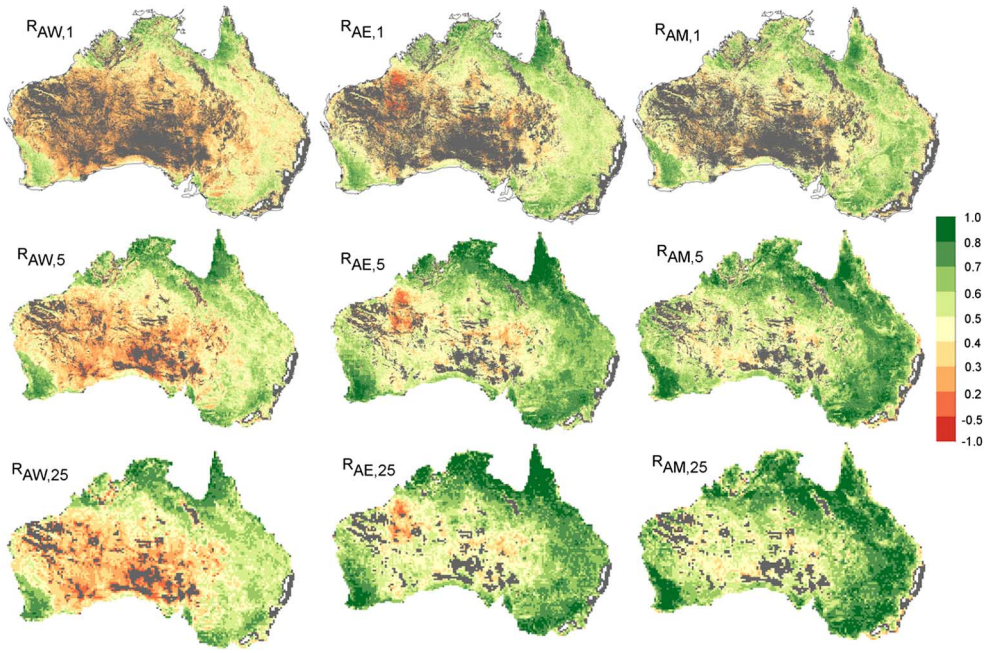

Fig. 10. Pearson correlation coefficient computed between ASAR GM and AWRA-L SSM (R_{AW}) (left), ERA-Interim (R_{AE}) (center), and AMSR-E SSM (R_{AM}) (right). The analyses were performed at 1 (upper line), 5 (center line), and 25 (lower line) km scale. The gray areas correspond to the nonsignificant correlation values ($\mathrm{p} > 0.05$) or missing values. The units represent the degree of saturation (%).

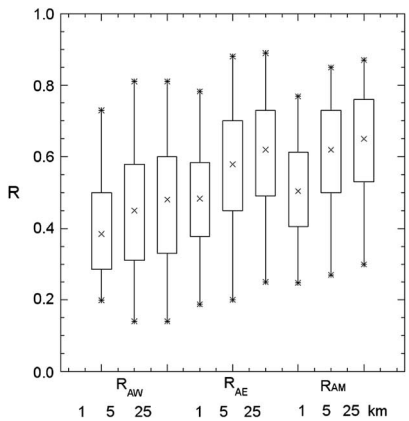

Fig. 11. Box-plot representation of quantities of the R maps computed from Fig. 10. The boxes show the median, 25th and 75th percentiles; the crosses represent the minimum and maximum R after outliers were removed.

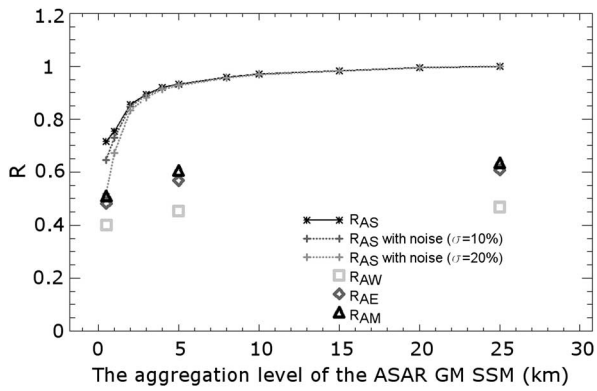

Fig. 12. Assessment of the spatial sampling error impact on R, approximated by R_{AS}, and its change with the ASAR GM SSM aggregation level (9) over 1500×1500 km area in southeastern Australia without (black line) and with introduced random noise ($\sigma = 10\%$ and $\sigma = 20\%$) (gray lines) overlaid with the continental mean of R_{AE}, R_{AW}, and R_{AM}.

This suggests a better suitability of R than RMSE to select the observations with the best benefit for data assimilation prior to the assimilation process itself. In particular, R should be neither too low nor too high. The former signifies large conceptual discrepancies in one or both SSM data or the fact that the data describe different phenomenon. The latter means that the model and observed SSM are almost identical. Both circumstances mean that improvement of modeled SSM via assimilation is unlikely.

The spatial sampling correlation $R_{AS,j}$ was estimated according to (9). The $1 - R_{AS,j}$ measure indicates the decrease from maximum $R = 1$ due to the spatial sampling error and noise. The $R_{AS,j}$ logarithmically increases (Fig. 12) with the increasing aggregation level j, but does so more rapidly than $R_{r,j}$. Already at 5 km, $R_{\mathrm{AS},5}$ reaches values above 0.9. By comparison, $R_{r,j}$ changes only minimally between different aggregation levels, suggesting that other error components (i.e., reference uncertainties) decreases $R_{r,j}$.

The impacts of noise and spatial sampling error on R at different ASAR GM aggregation levels (10) are shown in Fig. 13. The ΔsR_1 is more uniform when compared with the distinct patterns in the $\Delta\mathrm{sRMSE}_1$ difference maps (Fig. 6). Mean continental $n\Delta sR_1$ is also significantly lower than $\mathrm{n}\Delta\mathrm{sRMSE}_1$ (Fig. 9), which indicates that R is less impacted by spatial sampling error and noise than RMSE. The difference maps using other reference data (AMSR-E and ERA-Interim) showed very similar spatial patterns (not shown). This confirms that the difference method for R (10) depicts spatial sampling differences, with a negligible impact of reference uncertainty.

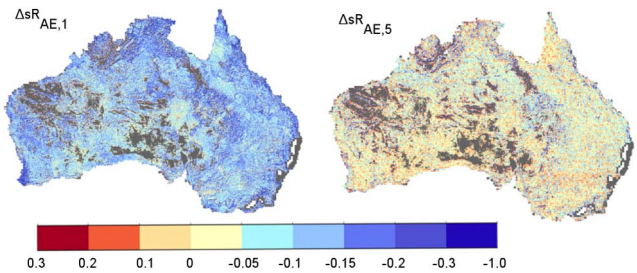

Fig. 13. Impact of the spatial sampling error and noise on R_{AE}. The gray areas correspond to the nonsignificant correlation values ($\mathrm{p} > 0.05$) or missing values.

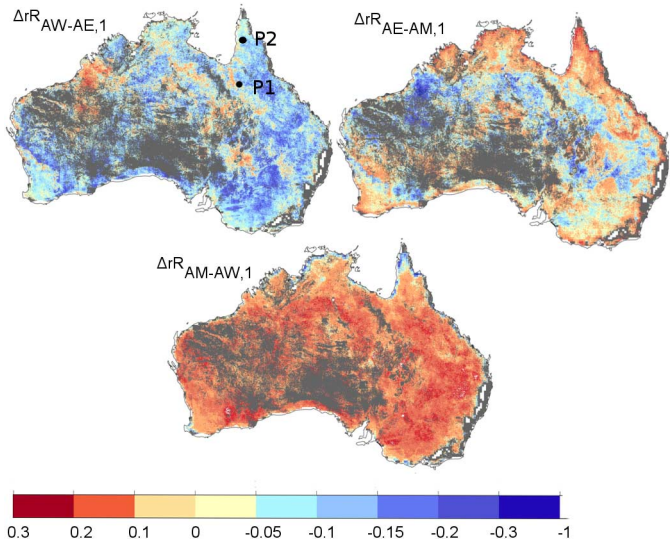

Fig. 14. Impact of the selection of the reference data on R at 1 km spatial resolution. The gray areas correspond to the nonsignificant correlation values ($\mathrm{p} > 0.05$) or missing values.

The effect on R due to the different reference data at 1 km (ΔrR_1) (11) is shown in Fig. 14. Similarly to RMSE, the spatial patterns did not change with the increasing ASAR GM aggregation levels while the absolute values slightly differed (data not shown). This supports the use of this difference method for the assessment of relative impact of reference uncertainty. The spatial patterns correspond to the $\Delta\mathrm{rRMSE}_1$ maps and the differences are most probably related to the simplifications in the models and different depths represented. Importantly, $n\Delta rR$ are significantly higher than $\mathrm{n}\Delta\mathrm{rRMSE}$ (Fig. 9) demonstrating a larger impact of reference uncertainity on R. In particular, the continental means $n\Delta rR$ are 12.9% at 1 km and 18.3% and 16.3% at 5 and 25 km spatial resolution, respectively. This compares to continental mean $\mathrm{n}\Delta\mathrm{rRMSE}$ equal to 4.3%, 9.8%, and 10.1% at 1, 5, and 25 km resolution. The regions where one reference data outperforms other may serve as a tool for model evaluation. For instance, the lower $R_{\mathrm{AM},1}$ when compared to $R_{\mathrm{AW},1}$ can be explained by the known limited performance of the AMSR-E SSM over coastal areas [29].

It becomes apparent that despite their noisy character at their native resolution, the ASAR GM SSM data accurately depict temporal soil moisture variability at resolution ≥ 2 km. Further averaging may slightly improve accuracy.

V. Conclusion

The performance of the ASAR GM SSM data was studied over the Australian continent by means of two widely used bivariate evaluation measures, RMSE and R. An important contribution beyond previous studies is that we perform the analyses at multiple scales and with different choices for reference data. This helps assess how, and at which scales, the spatial sampling error, noise and the choice of the reference data impact on RMSE and R. As such, this study explores the impact of spatial scale and reference data (extrinsic errors) and noise when evaluating medium resolution ASAR GM SSM product.

First, the spatial sampling error and noise were quantified using the spatial variance of the ASAR GM SSM within the coarser resolution (25 km) footprint as a proxy. The proportional share of noise in the latter was estimated by studying the differences between proxies computed using ASAR GM SSM with and without simulated random noise. Next, the spatial understanding of the effects due to spatial sampling error and noise on RMSE (R) was assessed by computing the differences between RMSE (R) maps acquired at finer (≤ 5 km) and coarser (25 km) resolutions. The important assumption is that the spatial variance differences between the ASAR GM 25 km aggregated product and the reference data can be neglected. Similarly, the effects due to different reference uncertainties were calculated as a difference between RMSE (R) maps using different reference data. Finally, to allow for a comparison of the separate error components, the calculated differences were normalized using the 25-km RMSE (R) maps. The subtraction method does not enable the actual quantification of the error components; it rather provides an estimate of how RMSE and R can differ under the impact of different error sources at different resolutions.

The results revealed large deviations in RMSE and R, depending on the spatial scale of aggregation and the choice of reference data, producing continental average values between 8% and 18% for the RMSE of relative soil moisture saturation and between 0.4 and 0.7 for R.

When compared to the 25 km sampling error- and noise-free RMSE map, the combined effect of noise and spatial sampling error accounted for a 79% RMSE increase at 1 km and a 13% increase at 5 km spatial resolution. In a simulated experiement, it was demonstrated that while a significant portion of the increase at 1 km originates from the ASAR GM noise, the change at 5 km is predominantly explained by the spatial sampling error. The effect of the uncertainty in the reference data on RMSE was lesser but not negligible (4.3%, 9.8%, and 10.1% normalized difference at 1, 5, and 25 km resolution, respectively). Our findings support the findings of [8] and [10] by showing that RMSE primarily reflects the random error and noise of the ASAR GM SSSM when computed at the original 1 km spatial resolution. Nevertheless, we showed that this dominance declines with the increasing ASAR GM aggregation level and that other error components become evident. Based on our results, it is suggested that a potential way for an improved ASAR GM SSM error assessment is to: 1) aggregate the data to ≥ 2 km resolution to minimize the

noise; 2) subtract the spatial sampling error within the coarse resolution footprint (e.g., using $\mathrm{RMSE}_{\mathrm{AS}}$ as a proxy) as performed in [26] for a soil moisture network; and 3) remove the reference uncertainty using more advanced techniques such as triple collocation [5].

The impact on R due to the choice of the reference data was larger than on RMSE and increased with spatial resolution (ranging between 12.9%, 18.3%, and 16.3% normalized difference at 1, 5, and 25 km resolution, respectively). As such it was more suitable to show how the observations and models change together and that with a minimal impact of spatial sampling error (4.8% at 5 km). This highlights the potential role of R to estimate the benefit of observations prior to data assimilation. In particular, R should be neither too low nor too high as both circumstances mean that improvement of modeled SSM via assimilation is unlikely.

Some additional conclusions can be drawn. 1) The RMSE hides the fact that the impact on the error is much stronger from relatively high versus from relatively low SSM values. This single evaluation measure may thus hide the actual origin of the uncertainty in the reference data. 2) The different bias correction method may produce slightly different spatial patterns in RMSE maps. The sensitivity of the fitting techniques is expected high for data with large level of noise, such as ASAR GM SSM. 3) Of interest may be further investigation on differences in RMSE maps if all data are bias corrected with respect to the reference data. 4) The method of RMSE and R map subtraction with different reference data enables the evaluation of the reference data themselves.

In the near future, satellites such as Sentinel-1 or SMAP will hopefully deliver soil moisture data at medium (1–9 km) spatial resolutions [31], [32] and improved radiometric accuracy. Of special interest is thus the transfer of our findings to the latter SAR missions.

References

[1] Y. Y. Liu *et al.*, "Developing an improved soil moisture dataset by blending passive and active microwave satellite-based retrievals," *Hydrol. Earth Syst. Sci.*, vol. 15, no. 2, pp. 425–436, 2011.

[2] A. W. Western and G. Blöschl, "On the spatial scaling of soil moisture," *J. Hydrol.*, vol. 217, pp. 203–224, 1999.

[3] A. W. Western, R. B. Grayson, and G. Bloschl, "Scaling of soil moisture: A hydrologic perspective," *Annu. Rev. Earth Planet. Sci.*, vol. 30, no. 1, pp. 149–180, 2002.

[4] R. Van der Velde, M. S. Salama, M. D. van Helvoirt, and Z. Su, "Decomposition of uncertainties between coarse MM5-Noah simulated and fine ASAR retrieved soil moisture over central Tibet," *J. Hydrometeorol.*, vol. 13, no. 6, pp. 1925–1938, 2012.

[5] W. Dorigo *et al.*, "Error characterisation of global active and passive microwave soil moisture datasets," *Hydrol. Earth Syst. Sci.*, vol. 14, no. 12, pp. 2605–2616, Dec. 2010.

[6] K. Scipal, T. Holmes, R. De Jeu, V. Naeimi, and W. Wagner, "A possible solution for the problem of estimating the error structure of global soil moisture data sets," *Geophys. Res. Lett.*, vol. 35, no. L24403, 2008.

[7] M. Doubkova, A. Bartsch, C. Pathe, D. Sabel, and W. Wagner, "The medium resolution soil moisture dataset: Overview of the SHARE ESA DUE Tiger project," in *Proc. IEEE Int. Symp. Geosci. Remote Sens.*, 2009, vol. 1, pp. I116–I119.

[8] C. Pathe, W. Wagner, D. Sabel, M. Doubkova, and J. Basara, "Using ENVISAT ASAR global mode data for surface soil moisture retrieval over Oklahoma, USA," *IEEE Trans. Geosci. Remote Sens.*, vol. 47, no. 2, pp. 468–480, Feb. 2009.

[9] I. Mladenova *et al.*, "Validation of the ASAR global monitoring mode soil moisture product using the NAFE'05 data set," *IEEE Trans. Geosci. Remote Sens.*, vol. 48, no. 6, pp. 2498–2508, Jun. 2010.

[10] M. Doubková, A. I. J. M. Van Dijk, D. Sabel, W. Wagner, and G. Blöschl, "Evaluation of the predicted error of the soil moisture retrieval from C-band SAR by comparison against modelled soil moisture estimates over Australia," *Remote Sens. Environ.*, vol. 120, pp. 188–196, 2012.

[11] A. Bartsch *et al.*, "Global monitoring of wetlands–the value of ENVISAT ASAR global mode," *J. Environ. Manage.*, vol. 90, no. 7, pp. 2226–2233, 2009.

[12] D. Sabel, Z. Bartalis, W. Wagner, M. Doubkova, and J.-P. Klein, "Development of a global backscatter model in support to the Sentinel-1 mission design," *Remote Sens. Environ.*, vol. 120, pp. 102–112, 2012.

[13] W. Wagner, G. Lemoine, M. Borgeaud, and H. Rott, "A study of vegetation cover effects on ERS scatterometer data," *IEEE Trans. Geosci. Remote Sens.*, vol. 37, no. 2, pp. 938–948, Mar. 1999.

[14] A. I. J. M. Van Dijk, *AWRA Technical Report 3. Landscape Model (version 0.5) Technical Description*. Canberra, Australia: WIRADA/CSIRO Water for a Healthy Country Flagship, 2010.

[15] A. I. J. M. Van Dijk and L. J. Renzullo, "Water resource monitoring systems and the role of satellite observations," *Hydrol. Earth Syst. Sci.*, vol. 15, no. 1, pp. 39–55, Jan. 2011.

[16] A. I. J. M. Van Dijk and S. Marvanek, *Derivation of a Simplified Soil Drainage Model. AWRA Background Paper 2010/1*. Canberra, Australia: WRADA/CSIRO Water for a Healthy Country Flagship, 2010.

[17] A. I. J. M. Van Dijk and G. A. Warren, *AWRA Technical Report 4. Evaluation Against Observations*. Canberra, Australia: WIRADA/CSIRO Water for a Healthy Country Flagship, 2010.

[18] M. Owe, R. A. M. De Jeu, and T. Holmes, "Multi-sensor historical climatology of satellite-derived global land surface moisture," *J. Geophys. Res.*, vol. 113, no. F01002, 2008.

[19] R. A. M. Jeu *et al.*, "Global soil moisture patterns observed by space borne microwave radiometers and scatterometers," *Surveys Geophys.*, vol. 29, no. 4–5, pp. 399–420, 2008.

[20] A. Simmons, S. Uppala, D. Dee, and S. Kobayashi, "ERA-Interim: New ECMWF reanalysis products from 1989 onwards," *ECMWF Newslett.*, vol. 110, pp. 25–35, 2007.

[21] D. P. Dee *et al.*, "The ERA-Interim reanalysis: Configuration and performance of the data assimilation system," *Q. J. Roy. Meteorol. Soc.*, vol. 137, no. 656, pp. 553–597, 2011.

[22] P. Viterbo and A. C. M. Beljaars, "An improved land surface parameterization scheme in the ECMWF model and its validation," *J. Clim.*, vol. 8, no. 11, pp. 2716–2748, 1995.

[23] R. H. Reichle and R. D. Koster, "Bias reduction in short records of satellite soil moisture," *Geophys. Res. Lett.*, vol. 31, no. 19501, pp. 1–4, 2004.

[24] L. Brocca *et al.*, "Improving runoff prediction through the assimilation of the ASCAT soil moisture product," *Hydrol. Earth Syst. Sci. Discuss.*, vol. 14, no. 10, pp. 1881–1893, 2010.

[25] W. Dorigo *et al.*, "The International soil moisture network: A data hosting facility for global in situ soil moisture measurements," *Hydrol. Earth Syst. Sci.*, vol. 15, no. 5, pp. 1675–1698, 2011.

[26] D. G. Miralles, W. T. Crow, and M. H. Cosh, "Estimating spatial sampling errors in coarse-scale soil moisture estimates derived from point-scale observations," *J. Hydrometeorol.*, vol. 11, no. 6, pp. 1423–1429, 2010.

[27] G. Kim and A. P. Barros, "Space-time characterization of soil moisture from passive microwave remotely sensed imagery and ancillary data," *Remote Sens. Environ.*, vol. 81, pp. 393–403, 2002.

[28] I. Rodriguez-Iturbe *et al.*, "On the spatial organization of soil moisture fields," *Geophys. Res. Lett.*, vol. 22, pp. 2757–2760, 1995.

[29] R. M. Parinussa *et al.*, "Error estimates for near-real-time satellite soil moisture as derived from the land parameter retrieval model," *IEEE Geosci. Remote Sens. Lett.*, vol. 8, no. 4, pp. 779–783, 2011.

[30] W. Wagner *et al.*, "Temporal stability of soil moisture and radar backscatter observed by the advanced synthetic aperture radar (ASAR)," *Sensors*, vol. 8, no. 2, pp. 1174–1197, 2008.

[31] M. Hornacek *et al.*, "Potential for high resolution systematic global surface soil moisture retrieval via change detection using sentinel-1," *IEEE J. Sel. Topics. Appl. Earth Observ. Remote Sens.*, vol. 5, no. 4, pp. 1303–1311, Aug. 2012.

[32] N. N. Das, D. Entekhabi, and E. G. Njoku, "An algorithm for merging SMAP radiometer and radar data for high-resolution soil-moisture retrieval," *IEEE Trans. Geosci. Remote Sens.*, vol. 49, no. 5, pp. 1504–1512, May 2011.

Marcela Doubková was born in Cheb, Czech Republic, in 1980. She received the M.A. degree in geography with specialization in cartography, remote sensing, and GIS from the University of Nebraska-Lincoln (UNL), Lincoln, NE, USA, in 2006, and the Ph.D. degree in natural science from the Vienna University of Technology, Vienna, Austria, in 2012.

From 2012 to 2013, she was a research fellow with the Earth Observation (EO) Science, Applications, and Future Technologies Department of the European Space Agency (ESA). Currently, she works as a Project Assistant at the Vienna University of Technology. Her research interests include microwave remote sensing of water in vegetation and soil and the application of derived microwave products in hydrological and crop modeling. In her dissertation, she provided a general approach for validation of remotely sensed soil moisture products with focus on soil moisture derived from SAR data. She has presented her research work at numerous conferences and meetings, and has published several conference and journal papers.

Dr. Doubkova is a Reviewer for the International Journal of Remote Sensing (IJRS), International Journal of Applied Earth Observation and Geoinformation, and Hydrology and Earth system Science (HESS) Journal.

Alena Dostálová was born in Hustopece, Czech Republic, in 1987. She received the B.Sc. degree in geodesy and cartography from the Technical University, Brno, Czech Republic, in 2010. She continues her Master studies at Vienna University of Technology, Vienna, Austria.

She works with the Institute of Geodesy and Geoinformation, Vienna University of Technology, in 2011. Her research interests include the soil moisture retrieval from SAR data.

Albert I. J. M. Van Dijk received the Master degree in science and the Ph.D. degree in philosophy from the Vrije University, Amsterdam, The Netherlands.

He is a Professor of Water Science and Management, Fenner School of Environment and Society, Acton, Australia. From 1996 to 2003, he was a Researcher at the VU University Amsterdam, Amsterdam, The Netherlands, studying aquifer hydraulic behavior; soil and nutrient conservation and catchment hydrology in Indonesia; the global carbon budget; and forest CO_2 exchange, as well as lecturing ecohydrology. From 2003 to 2012, he was a Research Scientist with CSIRO Land and Water, investigating the influence of land cover change on catchment health, salinity, and water resources; water resources availability and management in the Murray–Darling Basin; landscape remote sensing; environmental model-data fusion; and seasonal forecasting of water availability and drought. He has authored more than 130 publications. His research interests include hydrology, ecosystem biophysical functioning, environmental earth observation, and global change.

Prof. van Dijk led development of the Australian Water Resources Assessment (AWRA) system, a large computer system that underpins the Bureau of Meteorology's water accounts and reports by integrating satellite and on-ground observations with hydrological models of Australia's water balance in the recent years.

Günter Blöschl was born in Austria. He received a Diploma degree in civil engineering and the Ph.D. degree in hydrology from the Vienna University of Technology, Vienna, Austria.

From 1992 to 1994, he was a Research Fellow with the Centre for Resource and Environmental Studies, Australian National University, Canberra, Australia, and in 2007, he was appointed as a Full Professor of Hydrology and Water Resources, Vienna University of Technology. He is currently Director of the Doctoral Programme on Water Resource Systems, a multiyear inter-disciplinary Ph.D. programme at TU Vienna on water, focusing on biogeochemical and ecological processes impacting on water quality, and floods and droughts. He is the Author or Coauthor of more than 300 scientific articles on hydrology and earth system sciences, interdisciplinary water sciences, water resource systems, floods and droughts, hydrological modeling, and field experiments.

Prof. Blöschl is an Editor of Water Resources Research and other journals in the field. Recently, he received an Advanced Grant from the European Research Council (ERC) and the International Hydrology Award jointly from IAHS, UNESCO, and WMO.

Wolfgang Wagner (M'98–SM'07) was born in Wels, Austria, in 1969. He received the Dipl.Ing. (M.Sc.) degree in physics and the Dr.techn. (Ph.D.) degree in remote sensing, both with distinction, from Vienna University of Technology, Vienna, Austria, in 1995 and 1999, respectively.

In support of his M.Sc. and Ph.D. studies, he received fellowships to carry out research at the University of Berne, Berne, Switzerland; Atmospheric Environment Service Canada; NASA Goddard Space Flight Center; European Space Agency (ESA); and the Joint Research Center of the European Commission. From 1999 to 2001, he was with the German Aerospace Center (DLR), Germany. Since 2001, he has been a Professor of Remote Sensing with the Institute of Photogrammetry and Remote Sensing, Vienna University of Technology. His research interests include geophysical parameter retrieval techniques from remote sensing data, application development, active remote sensing techniques, particularly scatterometry, SAR, and full waveform airborne laser scanning.

Prof. Wagner has been a member of the ESA and EUMETSAT Science Advisory Groups for ASCAT, SMOS, and Sentinel-1. He was a Committee Chair of the European Geosciences Union Hydrologic Sciences Subdivision on Remote Sensing and Data Assimilation from 2005 to 2008. From 2008 to 2012, he was serving as a President of the International Society for Photogrammetry and Remote Sensing Commission VII (Thematic Processing, Modeling and Analysis of Remotely Sensed Data).

Diego Fernàndez-Prieto received the B.S. degree in physics from the University of Santiago de Compostela, A Coruña, Spain, in 1994, the Master degree in business administration (MBA) from the University of Deusto, Bilbao, Spain and the University of Kent, Kent, U. K, in 1997, and the Ph.D. degree in electronic engineering and computer science from the Department of Biophysical and Electronic Engineering, University of Genoa, Genoa, Italy, in 2001.

In 1994 and 1996, he was with the "Istituto per la Matematica Applicata" (I.M.A.), National Research Council (C.N.R.), Genoa, Italy. Since 2001, he has been with the Earth Observation (EO) Science, Applications and Future Technologies, Department of the European Space Agency (ESA). Currently, he is a Program Manager of the Support To Science Element (STSE), a scientific programme aimed at providing scientific support to both the formulation of novel mission concepts and the scientific exploitation of on-going ESA missions. His research activity is documented in more than 150 scientific publications.

Dr. Fernàndez-Prieto is a Reviewer for the journals IEEE TRANSACTIONS ON GEOSCIENCE AND REMOTE SENSING, Pattern Recognition Letters, Hydrogeology, Earth Science Informatics, Journal of Environmental Management, Remote and Remote Sensing of the Environment. He is also an Editor of several special issues in international peer-review journals: Journal of Environmental Management, Hydrology and Earth System Science, Geobioscience, Ocean Science and Remote Sensing.